ELSEVIER

Sensors and Actuators B 22 (1994) 227–236

SENSORS AND ACTUATORS B CHEMICAL

A gas sensor with porous films of $Bi_2Sr_2CaCu_2O_{8+x}$: an analysis of the response

X.J. Huang [a,1], J. Schoonman [a], L.Q. Chen [b]

[a] *Laboratory for Inorganic Chemistry, Julianalaan 136, 2628 BL Delft, Netherlands*

[b] *Institute of Physics, Academia Sinica, PO Box 603, Beijing 100080, China*

Received 7 September 1993; in revised form 13 June 1994; accepted 19 July 1994

Abstract

A systematic investigation has been carried out on the time dependence of the response to NO and CO of a gas sensor with a thick porous film of $Bi_2Sr_2CaCu_2O_{8+x}$ (BSCCO). The oxidation of reducing gases such as NO and CO by lattice oxygen occurs in parallel with desorption of NO_2 and CO_2, respectively, in the whole range of temperatures investigated. An extension of a reported model has been proposed in order to describe the response of the sensor. The time dependence of the electrical resistivity can be interpreted by assuming a conductivity dominated by Schottky barriers at grain boundaries. A kinetic model underlying the temperature dependence of the sensitivity to NO and the selectivity against CO is discussed. The high sensitivity to NO as compared to that to CO is attributed to the high adsorption rate of NO at low temperatures. The good selectivity at high temperatures is attributed to the rapid increase of the desorption rate of CO and/or CO_2 with increasing temperature. The response time increases with increasing equilibrium sensitivity S_0. The recovery time decreases with increasing S_0. They both decrease with increase of the desorption rate of CO(NO) and $CO_2(NO_2)$.

Keywords: BSCCO; Gas sensors

1. Introduction

The response behaviour of semiconductor gas sensors cannot be predicted by calculations based on thermodynamic data. A power law has been used to describe the relation between the conductance and the concentration of reducing gases for some semiconductor sensors. Several models have been reported to interpret this relation [1–9]. Some researchers have studied the response behaviour of thin-film sensors with thickness less than twice the Debye length [10–12]. Most of the reported studied present only experimental results and qualitative interpretations.

The response of semiconductor gas sensors can be due to a surface oxidation or reduction process, including adsorption of reducing species, electron exchange in parallel with oxygen exchange and desorption of a product. The investigation of the time dependence of the response is quite important to the understanding of the mechanism of a sensor. The basic kinetic parameters can be evaluated through this analysis using a model. Insight into the basic parameters, such as sensitivity, selectivity, response and recovery times, may lead to improved sensors, but may also lead to unravelling of the mechanism of heterogeneous catalysis.

To the best of our knowledge, only Clifford [13] and Pizzini et al. [5] have studied the kinetic behaviour quantitatively. Their results indicated an exponential variation of resistance in time when an n-type semiconductor sensor was exposed to reducing gases in air. When an n-type semiconductor is exposed to reducing gases, the gases react with surface-adsorbed oxygen such as O^- and/or O_2^-, and this is a fast process. Therefore, it is difficult to analyse the response curve in detail [4].

We have shown in a previous paper [14] that a thick (≈ 20 μm) layer of $Bl_2Sr_2CaCu_2O_{8+x}$ (BSCCO) on an Al_2O_3 substrate exhibits sensitivity to NO in NO_x–air mixtures. The lattice oxygen atoms in the surface layer participate in the reaction process. This is a relatively slow process, the response and recovery times being relatively long.

In this work, the kinetic behaviour of the response processes of a sensor based on a thick film of p-

[1] Present address: Group for Sensors and Solid State Ionics, Faculty of Technology, Christian-Albrechts University, Kaiserstrasse 2, D-24143 Kiel, Germany.

SSDI 0925-4005(94)01517-L

conducting $Bi_2Sr_2CaCu_2O_{8+x}$ with a 'Schottky-barrier-limited' conductance is analysed. When this sensor is exposed to a reducing gas, the adsorbed reducing gaseous species on the surface will react with a surface lattice oxygen, and subsequently desorbs. An equilibrium exists between the reducing gas, oxygen in the ambient and lattice oxygen in the surface layer. The concentration of lattice oxygens in the surface decreases. Therefore, the density of the electronic charge carriers, i.e., the holes, and hence the resistivity, will change.

An extension of the reported model will be used to describe the time dependence of the response and recovery of the sensor in reducing gases such as CO and NO. By making several assumption about the variables involved in the kinetic equations, a quasi-equilibrium approximation that predicts the response and recovery curves of the sensor is derived. The temperature dependence of the selectivity for NO against CO is discussed based on the kinetic data.

2. Theoretical considerations

In earlier reports [15], a sensing mechanism for the reducing gases CO and NO, or in general R, $Bi_2Sr_2CaCu_2O_{8+x}$ was proposed. The mechanism involves the following steps:

$$\mathrm{ad} + \mathrm{R} \underset{k_{-1}}{\overset{k_1}{\rightleftharpoons}} (\mathrm{R})_{\mathrm{ad}} \tag{1}$$

with ad an empty surface site, with an equilibrium constant $K_1 = k_1/k_{-1}$.

The interaction between $(R)_{ad}$ and a surface oxygen ion O_O^x is represented by

$$(\mathrm{R})_{\mathrm{ad}} + \mathrm{O}_{\mathrm{O}}^{\mathrm{x}} + 2\mathrm{h}^{\cdot} \underset{k_{-2}}{\overset{k_2}{\rightleftharpoons}} (\mathrm{RO})_{\mathrm{ad}} + \mathrm{V}_{\mathrm{O}}^{\cdot\cdot} \tag{2}$$

$(RO)_{ad}$ can desorb,

$$(\mathrm{RO})_{\mathrm{ad}} \underset{k_{-3}}{\overset{k_3}{\rightleftharpoons}} \mathrm{RO(g)} + \mathrm{ad} \tag{3}$$

Oxygen interact with the ceramic superconductor surface according to

$$\frac{1}{2}\mathrm{O}_2 + \mathrm{ad} \underset{k_{-4}}{\overset{k_4}{\rightleftharpoons}} \mathrm{O}_{\mathrm{ad}} \tag{4}$$

$$\mathrm{O}_{\mathrm{ad}} + \mathrm{V}_{\mathrm{O}}^{\cdot\cdot} \underset{k_{-5}}{\overset{k_5}{\rightleftharpoons}} \mathrm{O}_{\mathrm{O}}^{\mathrm{x}} + 2\mathrm{h}^{\cdot} \tag{5}$$

Eqs. (1) and (4) express the physical adsorption processes of the reducing gas R and O_2, respectively. They represent fast processes. Eq. (2) describes the oxidation of adsorbed species by lattice oxygen. Eqs. (3) and (5) represent product desorption and surface recovery processes, respectively.

The transition from physical adsorption to chemical adsorption of reducing gases (see Eq. (2)) is assumed to be a slow process and is the rate-determining step. $[(RO)_{ad}]$ can be calculated by considering the equilibrium of this process.

In the present study, the low sintering temperature of the ceramic layer, i.e., the poorly sintered case, leads to 'Schottky-barrier' contacts [15], as schematically shown in Fig. 1. At the contact area a Schottky barrier arises due to charge trapped in the surface states. In this case, conductivity will be limited by charge transport across the barrier. The temperature dependence of this 'Schottky-barrier-limited' conductivity is given by

$$\sigma \approx \text{constant} \times \exp(-eV_s/kT) \tag{6}$$

The conductivity activation energy is eV_s. The height variation of this barrier is ΔV_s, given by the Schottky equation for planar geometry, i.e.,

$$\begin{aligned}\Delta V_s &= [Q_s^2 - (Q_s^0)^2]/2\epsilon\epsilon_0 eN_A \\ &= (2Q_s^0\Delta Q_s + \Delta Q_s^2)/2\epsilon\epsilon_0 eN_A\end{aligned} \tag{7}$$

Here Q_s denotes surface charge, Q_s^0 denotes the surface charge in air and ΔQ_s is the change in surface charge due to adsorption of reducing gases. In this situation, $\Delta Q_s = 2nN_s[\mathrm{RO}]_{\mathrm{ad}}$ [16].

The time dependence of $(RO)_{ad}$ is given by

$$\begin{aligned}\frac{\mathrm{d}[(\mathrm{RO})_{\mathrm{ad}}]}{\mathrm{d}t} &= K_1 k_2 (\mathrm{O}_{\mathrm{O}}^{\mathrm{x}})[\mathrm{h}^{\cdot}]^2 P_{\mathrm{R}} - k_{-2}[(\mathrm{RO})_{\mathrm{ad}}][\mathrm{V}_{\mathrm{O}}^{\cdot\cdot}] \\ &\quad - k_3[(\mathrm{RO})_{\mathrm{ad}}]\end{aligned} \tag{8}$$

The gases flow through the chamber continuously during the period of the measurements, and it is assumed that the concentration of the reactant is constant and that the product is removed instantaneously. The boundary conditions are

$$P_{\mathrm{R}} = \text{constant} \tag{9}$$

$$[\mathrm{RO}] = 0$$

Eq. (8) can be rewritten as

$$\frac{\mathrm{d}[(\mathrm{RO})_{\mathrm{ad}}]}{\mathrm{d}t} = C_1 - C_2[(\mathrm{RO})_{\mathrm{ad}}] \tag{10}$$

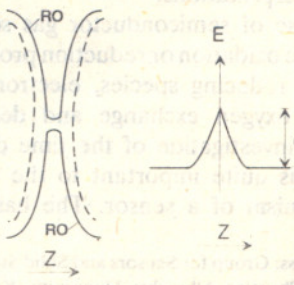

Fig. 1. Schematic of the 'Schottky-barrier-limited' contact.

$$k_1 k_2 P_R [O_O^x][h^\cdot]^2 \tag{11}$$

$$k_{-2}[V_O^{\cdot\cdot}] + k_3 \tag{12}$$

C_1 relates to the rate of chemisorption of a species and C_2 relates to the desorption rate and RO.

For low partial pressures of reducing gases and at temperatures, the coverage of adsorbed molecules low, and hence the concentrations $[O_O^x]$, $[h^\cdot]$ and are considered to be constant. Therefore, C_1 and can be taken as constant.

Fig. 2 shows typical response and recovery curves. $t=0$ the surface of a sensor is in equilibrium with The value of its resistivity in air is defined as the line. There is no chemical adsorption of the reducing $[(RO)_{ad}]=0$. After a relatively long exposure time, surface of the ceramic layer is in equilibrium with gas, hence $d[(RO)_{ad}]/dt=0$ and $[(RO)_{ad}]=C_1/C_2$. Integration of Eq. (10) and taking the boundary conditions into account yields (see Appendix 1).

$$[(RO)_{ad}] = \frac{C_1}{C_2} - \frac{C_1}{C_2}\exp(-C_2 t) \tag{13}$$

Substituting Eq. (13) into Eq. (7), and considering that $Q_s \ll Q_s^0$ and $\Delta Q_s = 2N_s[(RO)_{ad}]$ and N_s the number of acceptor states that can be ionized per unit volume, V_s can be expressed as

$$V_s = C\frac{C_1}{C_2} - C\frac{C_1}{C_2}\exp(-c_2 t) \tag{14}$$

with

$$C = N_s Q_s^0/\epsilon\epsilon_0 e N_A \tag{15}$$

The sensitivity S is defined as

$$S = \frac{\rho}{\rho_{air}} = \frac{\sigma_{air}}{\sigma} = \exp(\Delta V_s/kT) \tag{16}$$

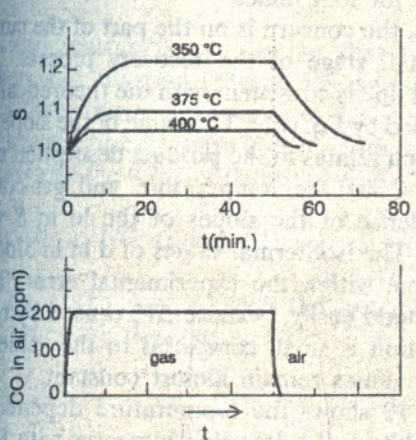

Fig. 2. Typical response and recovery curves of a sensor.

with ρ and σ the resistivity and conductivity of the sensor when exposed to reducing gases, and ρ_{air} and σ_{air} the resistivity and conductivity of the sensor in air as a reference, respectively.

Combining Eqs. (14) and (16) yields

$$\ln S = \frac{1}{kT}\left[C\frac{C_1}{C_2} - C\frac{C_1}{C_2}\exp(-C_2 t)\right] \tag{17}$$

The recovery process starts when the gas is replaced by air (i.e., Fig. 2) and is terminated when the resistivity of the sensor reaches the baseline value.

The partial pressure of the reducing gas become 0, and hence $(R)_{ad}=0$. Eq. (10) can then be replaced by

$$\frac{d[(RO)_{ad}]}{dt} = -C_2[(RO)_{ad}] \tag{18}$$

At $t=0$ the boundary condition reads $[(RO)_{ad}]=C_1/C_2$; when the surface of the sensor has recovered its original state in air and the resistivity recovered its baseline, the boundary conditions are $[(RO)_{ad}]=0$, and $d[(RO)_{ad}]/dt=0$.

Integration of Eq. (18) using these boundary conditions yields (see Appendix 2)

$$[(RO)_{ad}] = \frac{C_1}{C_2}\exp(-C_2 t) \tag{19}$$

$$\Delta V_s = C\frac{C_1}{C_2}\exp(-C_2 t) \tag{20}$$

$$\ln S = \frac{1}{kT}C\frac{C_1}{C_2}\exp(-C_2 t) \tag{21}$$

The description of the recovery process is based on the hypothesis that the rate of reaction (5) is higher than that of the product desorption. The rational for this hypothesis will be discussed later in Section 4.1.

3. Experimental

The starting powder of $Bi_2Sr_2CaCu_2O_{8+x}$ was prepared by the same method as described before [14]. Thick films were prepared by screen printing. Subsequently, the film was sintered at 600 °C in air for 20 h [15]. Ag paint was used to improve the electrical contact. The resistance of the sample was measured using a Keithley multimeter (847) and a Kipp & Zonen recorder (BD40). There is no obvious difference between the results of four-probe measurements and two-electrode measurements. This means that the contact resistance between the sample and Ag paste is much smaller than the resistance of the sample. The sample was exposed to gaseous ambients in a testing chamber that allows the gas flow to be controlled. The experimental set-up was described in more detail earlier [17]. The time dependence of the response of the sensor

upon exposure to and removal of NO and CO was measured in air at different temperatures.

4. Results and discussion

The resistivity of the sensor decreases with increasing temperature. It does not show bulk-limited behaviour because the ceramic material shows almost metallic conduction behaviour [17]. Instead, 'Schottky-barrier-limited' behaviour is observed [15].

4.1. Evaluation of the basic parameters of the response processes

4.1.1. The response process

From Eqs. (6), (7) and (10), and considering that $\Delta Q_s \ll Q_s^0$, one obtains

$$\frac{\mathrm{d}\ln S}{\mathrm{d}t} = \frac{1}{kT}\frac{\mathrm{d}(\Delta V_s)}{\mathrm{d}t} = C\frac{1}{kT}\frac{\mathrm{d}[(\mathrm{RO})_{ad}]}{\mathrm{d}t}$$

$$= C\frac{1}{kT}(C_1 - C_2[(\mathrm{RO})_{ad}]) \quad (22)$$

At $t=0$, $[(\mathrm{RO})_{ad}]=0$, and hence

$$\left.\frac{\mathrm{d}\ln S}{\mathrm{d}t}\right|_{t\to 0} = \frac{C}{kT}C_1 \quad (23)$$

In the initial stage, adsorbed R reacts on the surface with lattice oxygen. This causes a decrease of the hole concentration in the surface layer.

Combining Eqs. (11) and (23) yields

$$\left.\frac{\mathrm{d}\ln S}{\mathrm{d}t}\right|_{t\to 0} = \frac{C}{kT}K_1 k_2 P_R [O_O^x][h^\cdot]^2 \quad (24)$$

Figs. 3 and 4 show the ln S versus time curve of NO and CO at different temperatures, respectively. The values of d ln S/dt ($t\to 0$) for NO or CO under different partial pressures and at different temperatures are evaluated from these Figures. Tables 1 and 2 list the numerical data.

Figs. 5 and 6 show the d ln S/dt ($t\to 0$) versus P curves. They are straight lines, and this is consistent with the theoretical prediction expressed by Eq. (24). Their slopes are temperature dependent. The numerical values are listed in Tables 1 and 2, and represent $CeC_1/(kT)$. The value of C relates to the preparation conditions of the ceramic layer and temperature, and is independent of the nature of the gaseous species. The values of C_1 for different gaseous species can be evaluated from the values of these slopes.

From Eq. (11) it is predicted that C_1 is proportional to P_R when $[O_O^x]$ and $[h^\cdot]$ are constant. Therefore, d ln S/dt ($t=0$) is proportional to P_R.

Fig. 7 shows the temperature dependence of the slopes of the curves in Figs. 5 and 6. For both NO and CO, the values of $CeC_1/(kT)$ hardly vary from 300 to 400 °C. When the temperature increases to 450 °C, the value for NO decreases. The sensitivity to CO at 450 °C is very low, so it is difficult to record the kinetic response curve. There are five parameters that determine the change with temperature, i.e. C, K_1, $[O_O^x]$ and $[h^\cdot]$ decrease with increasing temperature, while k_2 increases with temperature. It is quite difficult to interpret the relation between the parameter values and the temperature. But at a fixed temperature, the value of C_1 for different gaseous species is proportional to the slope. Their values for NO are higher than those for CO. The relation between C_1 and the sensitivity and selectivity will be discussed later.

4.1.2. The recovery process

From Eq. (21) one obtains, taking the logarithm

$$\ln\ln S = \ln\left(\frac{C}{kT}\frac{C_1}{C_2}\right) - C_2 t \quad (25)$$

i.e., ln ln S should be proportional to the time.

Figs. 8 and 9 present ln ln S versus time curves for NO and CO, respectively. From Fig. 8(a) it is observed that the curves in the initial stage are straight lines. After a relatively long time, deviations from the straight lines occur. This can be attributed to oxygen diffusion in the material. During the response process, as the reducing gases adsorb on the surface, part of the lattice oxygen in the sub-surface layer will diffuse to the surface layer due to a concentration gradient. This process is slow. When the atmosphere is changed back to air, it takes quite some time to recover the lattice oxygen in the sub-surface layer, because the diffusion of oxygen ions in $Bi_2Sr_2CaCu_2O_{8+x}$ is rather slow at the operating temperature. The contribution of this process to the total sensitivity is quite small though. Within the initial few minutes, the ln ln S versus time curves are straight lines. Eq. (21) cannot be used to interpret the recovery process for long times.

Here, the concern is on the part of the curves during the initial stage of the recovery process. The initial straight line is consistent with the theoretical prediction expressed by Eq. (21). The value of the slope represents C_2, which relates to the product desorption rate. Tables 3 and 4 list the temperature and gas-concentration dependence of the slopes of the ln ln S versus time curves. The isothermal values of d ln ln S/dt are almost the same within the experimental error. This can be understood easily, because ΔV_s caused by reducing-gas adsorption is small compared to the value of V_s, k_{-1} and k_3 values remain almost constant.

Fig. 10 shows the temperature dependence of -d ln ln S/dt ($=C_2$). Its value increases with temperature, which is reasonable as the desorption rate increases with increasing temperature. The values for CO are

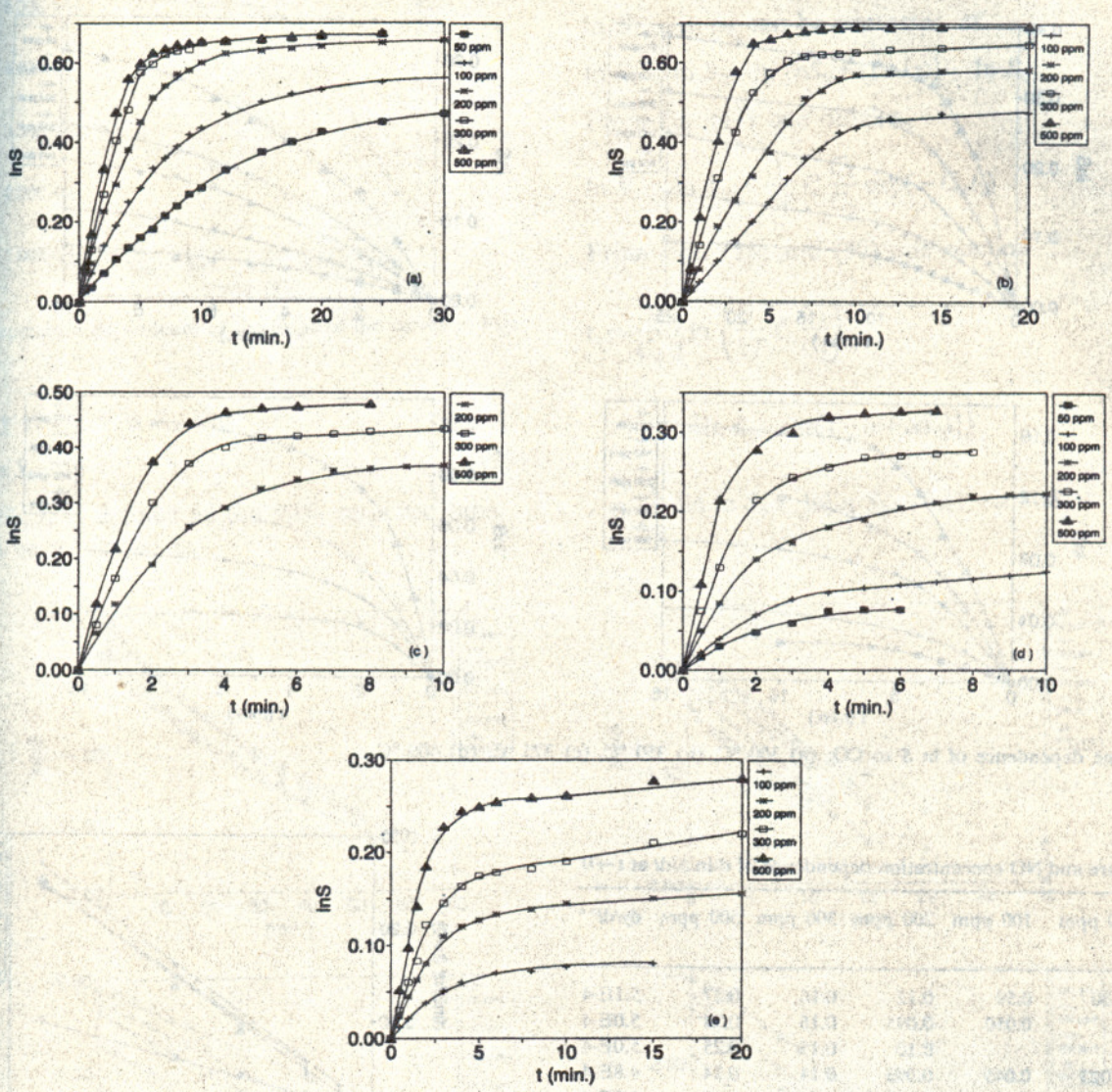

Fig. 3. Time dependence of ln S to NO: (a) 300 °C, (b) 350 °C, (c) 375 °C, (d) 400 °C, (e) 450 °C.

higher than those for NO, especially at high temperatures.

It is also reasonable to assume that the rate of desorption, i.e., reaction (3) and its inverse reaction, is slower than oxygen incorporation, i.e., reaction (5). The former reaction is, therefore, the rate-determining step. Otherwise the value of C_2 will be gas independent.

4.2. Selectivity to NO against CO

From Eq. (17) it can be seen that after long equilibration times the reduced reaction

$$\ln S_0 = \frac{C}{kT}\frac{C_1}{C_2} \tag{26}$$

holds, where S_0 is the equilibrium sensitivity and ln S_0 is proportional to $\exp(C_1/C_2)$.

From Tables 1 to 4, it can be concluded that the influence of temperature on C_1 is smaller than on C_2. The C_2 value for CO increases much faster than that for NO. Table 5 lists the $(C_1)_{NO}/(C_1)_{CO}$ and $(C_2)_{NO}/(C_2)_{CO}$ ratios at different temperatures. The values for $(C_1)_{NO}/(C_1)_{CO}$ are calculated from the values of the slopes of the curves in Figs. 3 and 4, which are listed in Tables 1 and 2. At low operating temperatures, the high sensitivity to NO is mainly attributed to the high C_1 value for NO. As the operating temperature increases, the sensitivity of CO will decrease quickly compared with than of NO; this is mainly attributed to the high C_2 value for CO. If the operating temperature increases, the selectivity for NO against CO will increase. However, the sensitivity will decrease. Therefore, there is an optimum temperature for practical utilization of the sensor.

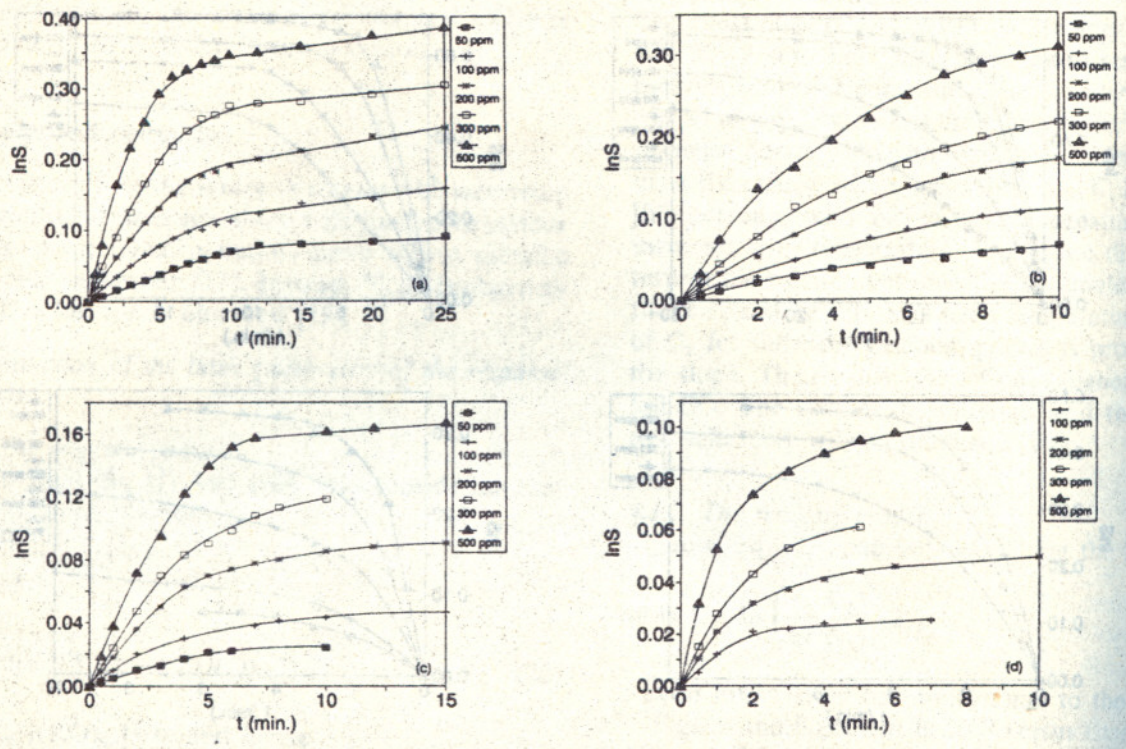

Fig. 4. Time dependence of ln S to CO: (a) 300 °C, (b) 350 °C, (c) 375 °C, (d) 400 °C.

Table 1
Temperature and NO concentration dependence of d ln S/dt at $t \rightarrow 0$

Temp. (°C)	50 ppm	100 ppm	200 ppm	300 ppm	500 ppm	dy/dP [a]
300	0.30	0.59	0.12	0.16	0.27	5.1E-4
350		0.050	0.095	0.16	0.24	5.0E-4
375			0.10	0.15	0.25	5.0E-4
400	0.023	0.045	0.093	0.14	0.24	4.8E-4
450		0.021	0.042	0.061	0.10	1.9E-4

[a] dy/dP is the value of the slope of the curve of d ln S/dt at $t=0$ vs. the partial pressure of gas.

Table 2
Temperature and CO concentration dependence of d ln S/dt at $t \rightarrow 0$

Temp. (°C)	50 ppm	100 ppm	200 ppm	300 ppm	500 ppm	dy/dP [a]
300	0.008	0.016	0.030	0.040	0.075	1.5E-4
350	0.011	0.025	0.035	0.048	0.068	1.3E-4
375	0.009	0.015	0.029	0.042	0.075	1.5E-4
400		0.013	0.028	0.41	0.065	1.4E-4

[a] dy/dP is the value of the slope of the curve of d ln S/dt at $t=0$ vs. the partial pressure of gas.

4.3. Response time

The response time t_r is defined as the time required for the sensor signal to reach a specified fraction α of the equilibrium value on exposure to the gases [6]. If the sensitivity is S_1 at time t_r, and the equilibrium

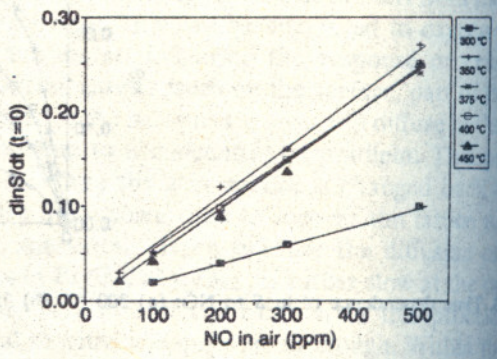

Fig. 5. NO partial-pressure dependence of the slopes of the plots of ln S vs. time at $t=0$.

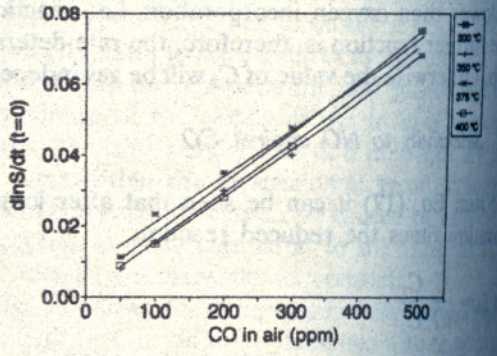

Fig. 6. CO partial-pressure dependence of the slopes of the plots of ln S vs. time at $t=0$.

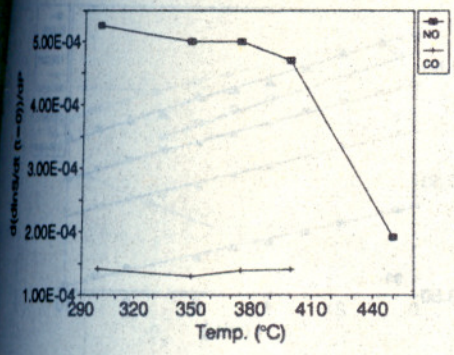

Fig. 7. Temperature dependence of the slope of the curves in Figs. 5 and 6.

sitivity at $t=\infty$ is S_0, then

$$S_1-1=\alpha(S_0-1) \tag{27}$$

If $\alpha=90\%$, t_r is defined as the 90% response time. S_1 can be expressed as

$$S_1=\alpha S_0+(1-\alpha) \tag{28}$$

$\ln S_1-\ln S_0$ can be expressed as

$$\ln S_1-\ln S_0=\ln[\alpha S_0+(1-\alpha)]-\ln S_0 \tag{29}$$

From Eq. (17) one obtains

$$\ln S_1-\ln S_0=\frac{1}{kT}C\frac{C_1}{C_2}\exp(-C_2t_1) \tag{30}$$

From Eqs. (26) and (30) one obtains

$$t_r=\frac{1}{C_2}\left\{\ln\left(\frac{1}{kT}C\frac{C_1}{C_2}\right)-\ln[\ln S_0-\ln(1-\alpha+\alpha S_0)]\right\}$$
$$=\frac{1}{C_2}\{\ln\ln S_0-\ln[\ln S_0-\ln(1-\alpha+\alpha S_0)] \tag{31}$$

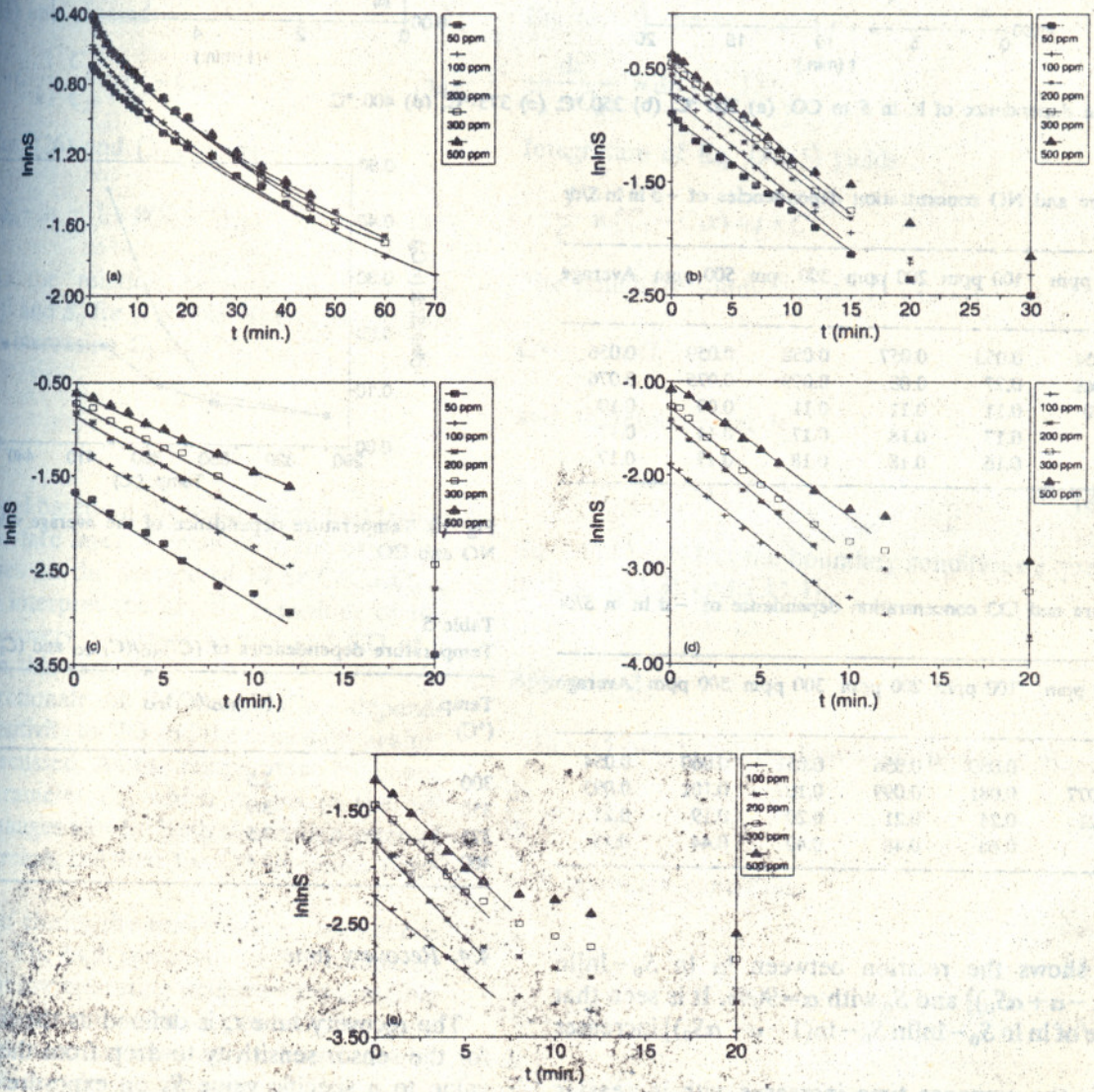

Fig. 8. Time dependence of ln ln S to NO: (a) 300 °C, (b) 350 °C, (c) 375 °C, (d) 400 °C, (e) 500 °C.

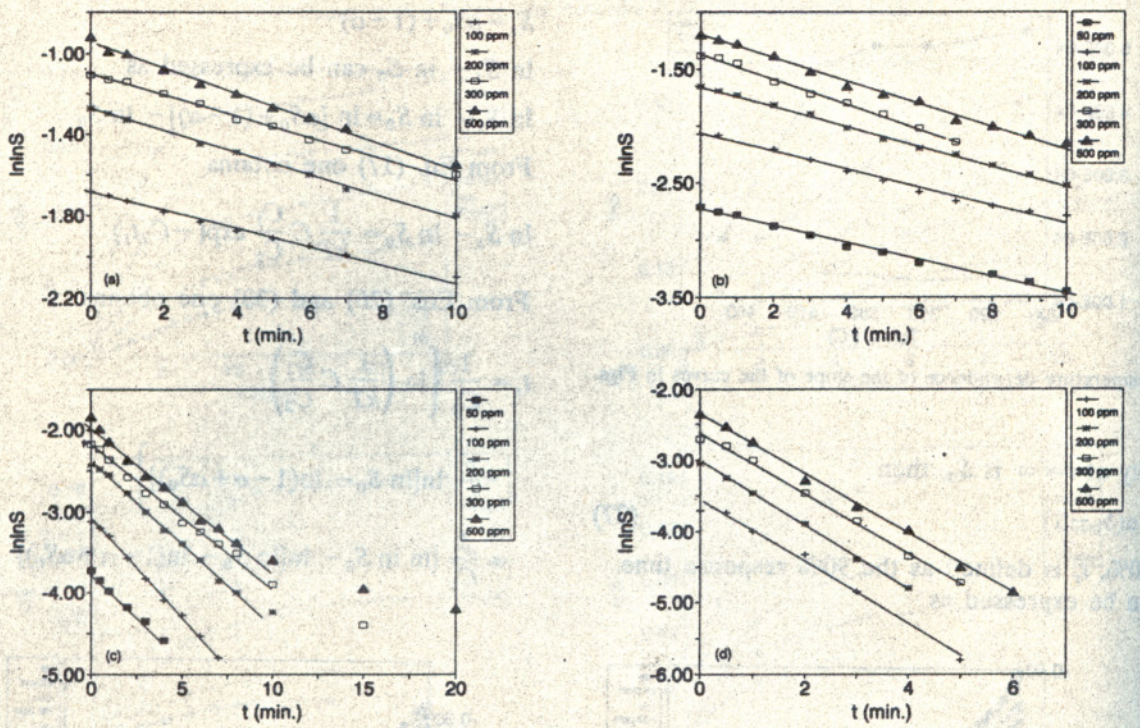

Fig. 9. Time dependence of ln ln S to CO: (a) 300 °C, (b) 350 °C, (c) 375 °C, (d) 400 °C.

Table 3
Temperature and NO concentration dependencies of $-\mathrm{d}\ln\ln S/\mathrm{d}t$ $(=C_2)$

Temp. (°C)	50 ppm	100 ppm	200 ppm	300 ppm	500 ppm	Average
300	0.051	0.053	0.057	0.058	0.059	0.056
350	0.069	0.77	0.08	0.079	0.075	0.076
375	0.10	0.11	0.11	0.11	0.09	0.10
400		0.17	0.18	0.17	0.14	0.17
450		0.16	0.18	0.18	0.17	0.17

Table 4
Temperature and CO concentration dependence of $-\mathrm{d}\ln\ln S/\mathrm{d}t$ $(=C_2)$

Temp. (°C)	50 ppm	100 ppm	200 ppm	300 ppm	500 ppm	Average
300		0.050	0.056	0.051	0.060	0.054
350	0.077	0.081	0.099	0.107	0.101	0.093
375	0.21	0.24	0.21	0.20	0.19	0.21
400		0.46	0.48	0.40	0.44	0.45

Fig. 11 shows the relation between $\ln\ln S_0 - \ln[\ln S_0 - \ln(1-\alpha+\alpha S_0)]$ and S_0 with $\alpha = 90\%$. It is seen that the value of $\ln\ln S_0 - \ln[\ln S_0 - \ln(1-\alpha+\alpha S_0)]$ increases with S_0.

Hence, the response time increases with increasing S_0 and decreases with increasing value of C_2.

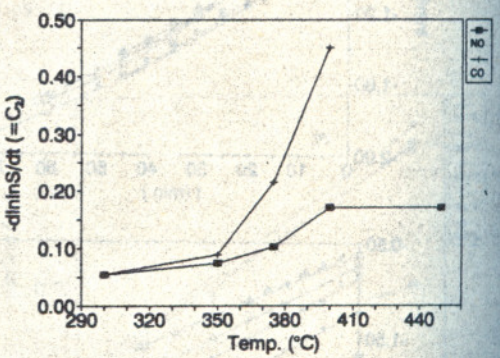

Fig. 10. Temperature dependence of the average values of C_2 for NO and CO.

Table 5
Temperature dependencies of $(C_1)_{NO}/(C_1)_{CO}$ and $(C_2)_{NO}/(C_2)_{CO}$

Temp. (°C)	$(C_1)_{NO}/(C_1)_{CO}$	$(C_2)_{NO}/(C_2)_{CO}$
300	3.5	1.0
350	3.9	0.82
375	3.5	0.50
400	3.4	0.37

4.4. Recovery time

The recovery time t_c is defined as the time required for the sensor sensitivity to drop from the equilibrium value to a specific value S_2 on exposure to inert gas [6]. S_2 is related to S_0:

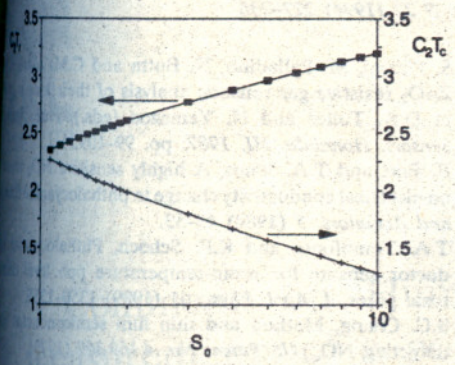

11. Curves of ln ln S_0 − ln[ln S_0 − ln(1−α+αS_0)] (=C_2t_r) and t_c − ln ln[1+β(S_0−1)] (=C_2t_c) vs. S_0.

$$-1=\beta(S_0-1) \tag{32}$$

β=10%, t_c is the 90% recovery time.
om Eq. (32), S_2 can be expressed as

$$+1+\beta(S_0-1) \tag{33}$$

m Eq. (21) one obtains

$$t_c-\ln S_0=C\frac{1}{kT}\frac{C_1}{C_2}\exp(-C_2t_c) \tag{34}$$

bining Eqs. (26) and (34) yields

$$\frac{1}{C_2}\{\ln\ln S_0-\ln\ln[1+\beta(S_0-1)]\} \tag{35}$$

g. 11 shows the relation between ln ln S_0 − ln +β(S_0−1)] and S_0 for β=10%. The recovery time reases with increasing C_2 and S_0.

Conclusions

kinetic model based on the assumption that lattice gen in the surface layer is involved in the oxidation educing gases on the surface of $Bi_2Sr_2CaCu_2O_{8+x}$ be used to interpret the kinetic behaviour of the ponse and recovery processes to NO and CO of a sor based on this material.

The kinetic rationale of the temperature depend- ces of the sensitivity to NO and the selectivity against has been discussed. As the temperature increases, value of parameter C_1, which relates to the ad- ption rate, changes slowly. Both desorption rates of and CO increase, but that for CO increases more idly.

t is difficult to clarify the temperature dependence he sensitivity. The high sensitivity to NO compared h that to CO at low operating temperatures is mainly ibuted to the high adsorption rate of NO. The good ctivity at high temperatures is attributed to the id increase of the desorption rate of CO and/or at increasing temperatures.

The response time increases with increasing S_0 and the recovery time decreases with increasing S_0. They both decrease with the desorption rate of R and RO.

Appendix 1

Eq. (13) will be derived starting Eq. (10):

$$\frac{dx}{dt}=C_1-C_2x \tag{A1.1}$$

with boundary conditions

$$x|_{t=0}=0 \tag{A1.2}$$

$$x|_{t=\infty}=\frac{C_1}{C_2} \tag{A1.3}$$

$$\left.\frac{dx}{dt}\right|_{t=\infty}=0 \tag{A1.4}$$

Eq. (A1.1) can be rewritten as

$$\frac{dx}{C_1-C_2x}=dt \tag{A1.5}$$

Integration of Eq. (A1.5) yields

$$-\frac{1}{C_2}\ln(C_1-C_2x)=t+C \tag{A1.6}$$

The boundary condition (A1.2) reveals

$$C=\frac{1}{C_2}\ln C_1 \tag{A1.7}$$

and, therefore, x reads

$$x=\frac{C_1}{C_2}-\frac{C_1}{C_2}\exp(-C_2t) \tag{A1.8}$$

Eq. (A1.8) satisfies the boundary conditions expressed in Eqs. (A1.3) and (A1.4).

Appendix 2

Eqs. (19)–(21) will be derived starting from Eq. (18):

$$\frac{dx}{dt}=-C_2x \tag{A2.1}$$

with boundary conditions

$$x|_{t=0}=\frac{C_1}{C_2} \tag{A2.2}$$

$$x|_{t=\infty}=0 \tag{A2.3}$$

$$\left.\frac{dx}{dt}\right|_{t=\infty}=0 \tag{A2.4}$$

Eq. (A2.1) can be rewritten as

$$\frac{dx}{-C_2x} = dt \tag{A2.5}$$

Integration of Eq. (A2.5) yields

$$-\frac{1}{C_2}\ln x = t + C \tag{A2.6}$$

The boundary condition (A2.2) reveals

$$C = -\frac{1}{C_2}\ln\left(\frac{C_1}{C_2}\right) \tag{A2.7}$$

and, hence, x reads

$$x = \frac{C_1}{C_2}\exp(-C_2t) \tag{A2.8}$$

Eq. (A2.8) satisfies the boundary conditions expressed in Eqs. (A2.3) and (A2.4).

References

[1] R.B. Copper, G.N. Advani and A.G. Jordan, Gas sensing mechanisms in tin dioxide thin films, *J. Electron. Mater., 10* (1981) 455–472.

[2] G. Sberveglieri, S. Groppelli and G. Coccoli, Radio frequency magnetron sputtering growth and characterization of indium–tin oxide (ITO) thin films for NO_2 gas sensors, *Sensors and Actuators, 15* (1988) 235–242.

[3] G. Sberveglieri, P. Benussi, G. Coccoli and P. Nelli, Reactively sputtered indium tin oxide polycrystalline thin film as NO and NO_2 gas sensors, *Thin Solid Films, 186* (1990) 349–360.

[4] S.C. Chang, Thin-film semiconductor NO_x sensor, *IEEE Trans. Electron Devices, ED-26* (1979) 1875–1880.

[5] S. Pizzini, M. Palladino, N. Butta and C.M. Mari, Thick film ZnO_2 resistive gas sensors, analysis of their kinetic behaviour, in D.R. Tuller and N. Yamazoe (eds.), *Proc. Symp. Chem. Sensors, Honolulu, HI, 1987,* pp. 99–109.

[6] B. Bott and T.A. Jones, A highly sensitive NO_2 sensor based on electrical conductivity change in phthalocyanine films, *Sensors and Actuators, 5* (1984) 43–53.

[7] T.A. Temofonte and K.F. Schoch, Phthalocyanine semiconductor sensors for room-temperature ppb level detection of toxic gases, *J. Appl. Phys., 65* (1989) 1350–1355.

[8] S.C. Chang, Method and thin film semiconductor sensor for detecting NO_x, *US Patent No. 4 169 369* (1979).

[9] P.K. Clifford and D.T. Tuma, Characteristics of semiconductor gas sensors, I. Steady state gas response, *Sensors and Actuators, 3* (1982/1983) 233–254.

[10] H. Windischmann and P. Mark, A model for the operation of a thin-film SnO_x conductance-modulation carbon monoxide sensor, *J. Electrochem. Soc., 126* (1979) 627–633.

[11] L. De Angelis and N. Minnaja, Sensitivity and selectivity of a thin-film tin oxide gas sensor, *Sensors and Actuators B, 3* (1991) 197–204.

[12] S. Strässler and A. Reis, Simple models for n-type metal oxide gas sensors, *Sensors and Actuators, 4* (1983) 465–472.

[13] P.K. Clifford, Homogeneous semiconducting gas sensor: a comprehensive model, in T. Seiyama, K. Fueki, J. Shiokawa and S. Susuki (eds.), *Proc. Int. Meet. Chemical Sensors, Fukuoka, Japan, 1983,* pp. 135–146.

[14] X.J. Huang, L.Q. Chen and J. Schoonman, High T_c superconductors as NO_x and CO_x sensor materials, *Solid State Ionics, 57* (1992) 7–10.

[15] X.J. Huang and J. Schoonman, Mechanism of a 'Schottky barrier-limited' $Bi_2Sr_2CaCu_2O_{8+x}$-based sensor for CO and NO_x, *Sensors and Actuators B, 22* (1994) 219–226.

[16] X.J. Huang, Superconductors in chemical devices, *Ph.D. Thesis*, Delft University of Technology, The Netherlands, 1993.

[17] R.J. Cava, B. Batlogg, S.A. Sunshine, T. Siegrist, R.M. Fleming, K. Rabe, L.F. Schneemeyer, D.W. Murphy, R.B. van Dover, P.K. Gallagher, S.H. Glarum, S. Nakahara, R.C. Farrow, J.J. Krajewski, S.M. Zahurak, J.V. Waszczak, J.H. Marshall, P. Marsh, L.W. Rupp, Jr., W.F. Peck and E.A. Retman, Studies of oxygen-deficient barium copper yttrium oxide ($Ba_2YCu_3O_{9-x}$) and superconductivity of bismuth(lead)–strontium–calcium–copper oxide, *Physica, C* 153–155 (1988) 560–565.